IRAQI JOURNAL OF MATERIALS
Volume (4) Issue (1) January-March 2025, pp. 17-22

Hydroxyapatite Powder Prepared by Sol-Gel Method for Biomedical Applications

Inaam M. Abdulmajeed [1], Suha H. Ibraheem [2]

[1] *Department of Physics, College of Science, University of Baghdad, Baghdad, IRAQ*
[2] *College of Basic Education, Mustansiriyah University, Baghdad, IRAQ*

Abstract
This investigation is focused on the production of hydroxyapatite (HA) powder and the impact of calcination temperature on the crystalline structure of HA. This work involved the chemical synthesis of HA powder utilizing stoichiometric ratios of the initial ingredients, followed by gel formation, drying, crushing, and calcination at temperatures ranging from 600°C to 800°C. Samples sintered at 600°C and 800°C were examined for their mechanical characteristics, such as Vickers microhardness and Young's modulus. The results demonstrated that higher sintering temperatures improved crystallinity and stiffness via increasing microhardness and Young's modulus. The synthetic HA powder's polycrystalline nature was confirmed by x-ray diffraction (XRD) examination, with the main peak exhibiting the maximum crystallinity. Debye-equation Scherrer's formula was used to get the average crystallite size. The investigation of hydroxyapatite functional groups using Fourier-transform infrared spectroscopy (FTIR) revealed distinctive peaks.

Keywords: Hydroxyapatite; Biomaterials; Bioceramics; Microstructure; Sol-gel
Received: 20 August 2024; **Revised:** 22 October 2024; **Accepted:** 29 October; **Published:** 1 January 2025

1. Introduction

In biological systems, the primary inorganic element in the structure of bones and teeth is hydroxyapatite (HA). In 1981, HA was used for the first time to treat a periodontal lesion, which has the same meaning as the term "periodontal", which refers to the area of dentistry that deals with the framework that supports and surrounds teeth. A lesion is a section of an organ or tissue that has been harmed by trauma or illness. In the medical field, HA is widely used and its applications have grown to include films, solid blocks, and solid components for dental implants [1]. Due to its exceptional biocompatibility, calcium phosphate has undergone substantial research for potential biomedical applications, numerous investigations have demonstrated that HA ceramics have the potential to connect directly to the host bone and exhibit no toxicity, inflammation, pyrogenetic reaction, or fibrous tissue formation [2].

In recent years, researchers working in the field of biomaterials have been interested in hydroxyapatite $Ca_{10}(PO_4)_6(OH)_2$, as an essential inorganic biomaterial [3,4]. On the basis of crystallographic and chemical research, it is known that synthetic HA and naturally occurring HA are comparable. Different methods can be used to prepare HAp particles such as modified precipitation [5,6], hydrothermal [7], and sol-gel [8]. The microstructural characteristics of HAp, including sintered density, grain size, grain size distribution, and microstructural flaws, heavily influence their mechanical performance. In order to create ceramic HAp with a high sintered density and suitable microstructure, the preparation of fine and well-calcination temperature of HAp powder is the most crucial stage [9].

The main objective of this work is to synthesize hydroxyapatite powder by sol-gel method and study the effect of calcination temperature on the crystalline structure to obtain a high degree of crystallinity and purity of HA powder which may be developed later to use in a biomedical applications. Mechanical properties such as Vickers microhardness and Young's modulus for the prepared samples were studied as a function of sintering temperature.

2. Experimental Work

The chemicals such as Ca $(NO_3)_2.4H_2O$ supplied by Himedia with 99.5% purity and P_2O_5 with 99% purity were used as starting materials. Stoichiometric ratios for each component were used to prepare

$Ca_{10}(PO_4)_6.(OH)_2$. Each compound was dissolved in 100 ml of ethanol, then both solutions were slowly mixed using magnetic stirrer for 20 minutes until the formation of a gel. The prepared gel was dried in an electric oven at 70°C for 20 hours. The prepared compound was crushed in agate mortar and calcined at temperature of 600 to 800°C with heating rate of 5°C/min for 3 hours. The powders were finally cooled by switching off the furnace to room temperature.

The mechanical properties such as Vickers microhardness and Young's modulus of the prepared hydroxyapatite samples were studied as functions of sintering temperature.

According to the hexagonal crystallite structure of hydroxyapatite, the lattice constant parameters were calculated by [10,11]

$$\frac{1}{d^2} = \frac{4}{3}\left[\frac{h^2+k^2+hk}{a^2}\right] + \frac{l^2}{c^2} \quad (1)$$

where *hkl* are Miller indices of crystal plane, *d* denotes the distance between neighboring planes, and the lattice constants were determined to be *a*=*b*=9.4116 and *c*=6.11

The following Debye-Scherrer's formula was used to determine the average crystallite size [12]:

$$D = \frac{0.9\lambda}{\beta\, cos\theta} \quad (2)$$

The following formula was employed to determine the volume of a hexagonal unit cell in hydroxyapatite [11,12]:

$$V = 2.589a^2c \quad (3)$$

The specific surface area of hydroxyapatite was calculated using the following formula:

$$S = \frac{6\times10^3}{D\times\rho} \quad (4)$$

where *D* is the crystallite size, and *ρ* is the theoretical density of HAp (3.16 g/cm^3)

A special hardness instrument is normally used to conduct the Vickers hardness test on the prepared Hap samples placed on the stage of the testing device. A load of 1 kg was applied to imprint a diamond tip. The device will press down on the sample's surface for a predetermined amount of time (often 10 to 30 s). Once the load is released, the two diagonals (d_1 and d_2) of the indentation are measured using a built-in optical microscope in the testing device. The measurement was repeated many times for sake of accuracy. The Vickers hardness number (H_V) is determined by the following formula [13]:

$$H_v = 1.854 \times \frac{F}{(d_1\times d_2)} \quad (5)$$

where *F* is the applied load in kilograms

The ASTM standard D2845-08 is used to perform the V-Meter MK IV ultrasonic instrument.

The following equation was used to compute elastic modulus [14]:

$$E = \frac{V_L^2\rho(1+\gamma)(1-2\gamma)}{1-\gamma} \quad (6)$$

where *E*, *ρ*, and V_L are respectively the elastic modulus, bulk density, ultrasonic longitudinal wave velocity

$$\gamma = \frac{1-2(\frac{v_T}{v_L})^2}{2-2(\frac{V_T}{V_L})^2} \quad (7)$$

where V_T and V_L are transverse and longitudinal velocity, respectively

With fracture toughness defined as the material's resistance to crack propagation, an empirical relationship between hardness and fracture toughness is utilized by indentation fracture toughness technique. The Vickers indent and cracks profile were observed under an optical microscope on the surface of prepared sample in order to determine the precise values of the fracture lengths. The Vickers hardness (H_V) and fracture toughness (K_{IC}) of a material are related by the indentation fracture toughness equation, which is a frequently used correlation. This method proposed by Antis et al. [15] offers an estimation of fracture toughness as

$$K_{IC} = 0.0161 \times (\frac{E}{H_v})^2 \times \frac{P}{C^{1.5}} \quad (8)$$

A load of 50 N was used in this work. It is reasonable to infer that the created cracks will always have a half-penny median crack profile. This suggests that only an equation specifically appropriate for half-penny median cracks should be used for this study in order to calculate K_{IC}. Figure (1) shows the profile of half-penny median, which typically develops at low indentation loads. This type of cracks combines with the cracks at the indent's corner to create the radial-median crack by diffusing beneath the indent [16].

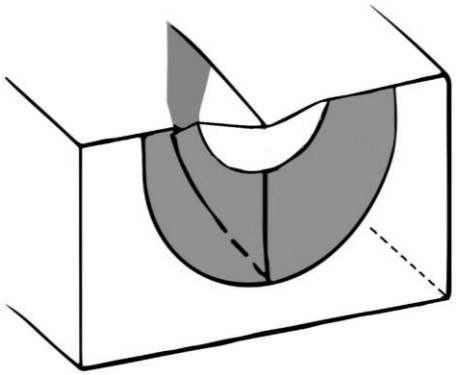

Fig. (1) A radial-median crack brought on by the Vickers load

3. Results and Discussion

Figure (2) illustrates the XRD patterns for the samples prepared at 600 and 800°C. The scanning range of diffraction angle (2θ) was 10-80° for all samples. By comparing between the resulting patterns and tabulated data of HA for 2θ, peak intensity, and Miller indices with the International Centre for Diffraction Data (ICDD) card no. 96-431-7044, it is clear that the prepared hydroxyapatite $Ca_{10}(PO_4)_6.(OH)_2$ powder is polycrystalline and the highest peak on the pattern corresponds to the highest plane crystallinity.

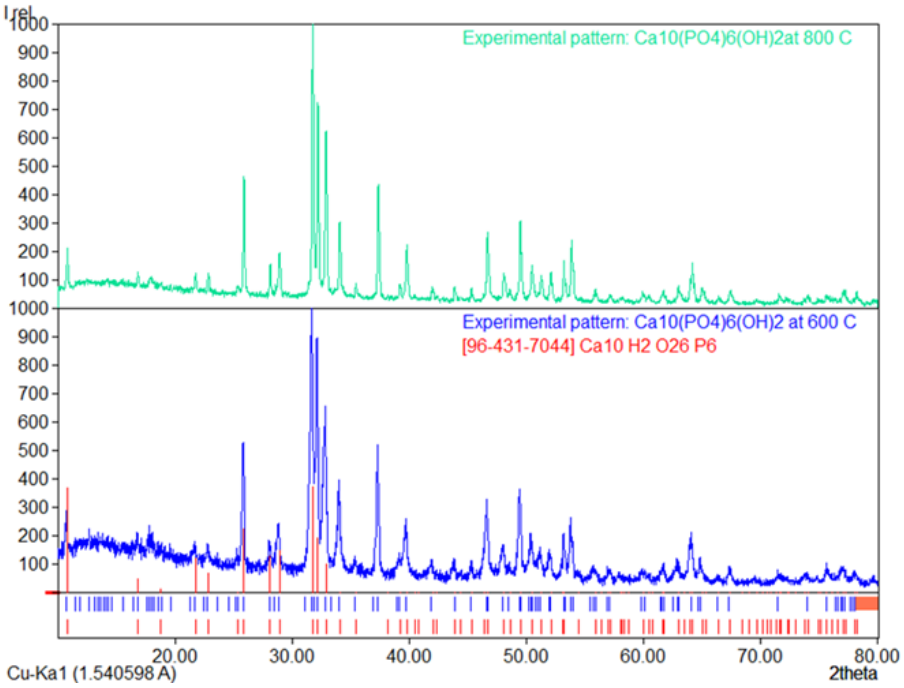

Fig. (2) XRD patterns of HAp powder prepared at 600 and 800°C

Debye-Scherrer's formula was used to determine the average crystallite size of Hap prepared at 800°C to be 36.27 nm. Equation (3) was used to calculate the hexagonal unit cell volume of the HAp structure to be 1365.5203. It was found that the specific surface area (S) was 52.349 using Eq. (4).

The FTIR spectra of HA powder prepared at 600 and 800 °C, respectively, are shown in figures (3) and (4). It is clear that the vibrational and stretching modes of the hydroxyapatite -OH groups have generated the peaks at 634 and 3571 cm^{-1}. The peaks seen at 468, 567, 603, 960, and 1039-1093 cm^{-1} are attributed to the distinctive tetrahedral structure of PO_4^{-3}. The PO_4^{-3}(2υ) and PO_4^{-3}(4υ) modes are represented by the peaks at 468 and 567 cm^{-1}, respectively. Additionally, PO_4^{-3}(3υ) mode is responsible for the peak seen at 960 cm^{-1}, while the PO_4^{-3}(1υ) mode is responsible for the peaks seen at 1093 and 1039 cm^{-1} [17].

ISSN (print) 2958-8960 (online) 3006-6042 Printed in IRAQ

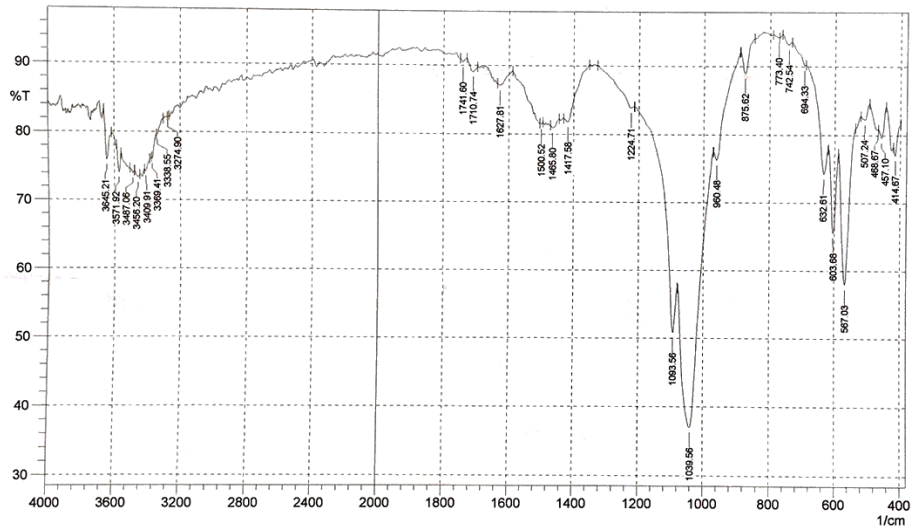

Fig. (3) FTIR spectrum of HA powder prepared at 600°C

Figure (4) shows a sharp peak at 3509 cm^{-1} and a medium peak at 634 cm^{-1} due to the stretching and vibrational, respectively, modes of the –OH groups of hydroxyapatites. The medium peaks seen at 1461 and 1417 cm^{-1} are ascribed to the CO_3^{-2} group. These peaks show that the PO_4^{-3} group in the HA lattice has been replaced by the CO_3^{-2} group, which may have begun when ambient carbon dioxide was adsorbed [18]. Therefore, it is clear that the synthetic powder is unquestionably hydroxyapatite.

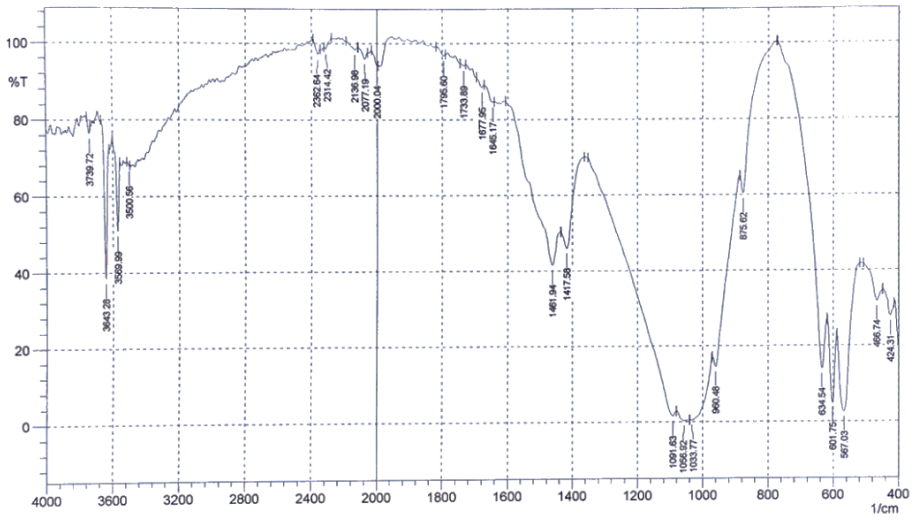

Fig. (4) FTIR spectrum of HA powder prepared at 800°C

The grain size of pure HAp was also measured using the field-emission scanning electron microscopy (FE-SEM). The concept that temperature-dependent development of crystallite size occurring in the prepared samples was based on the surface morphology introduced by FE-SEM. This can be used to explain why these microstructures of derived HAp form during the thermal process since particles have a tendency to crystallize and congregate at high temperatures. Figure (5a) illustrates how the prepared HAp crystallized into nanoparticles with sizes between 14 and 49nm at 600°C. As the preparation temperature was increased to 800°C, HAp microstructures became more apparent (Fig. 5b). The crystallite size of the prepared HAp varies from 40 to 60 nm.

The FE-SEM microimages make it easy to see changes in the grain size and semi-spherical shape as the grain size increased with increasing preparation temperature.

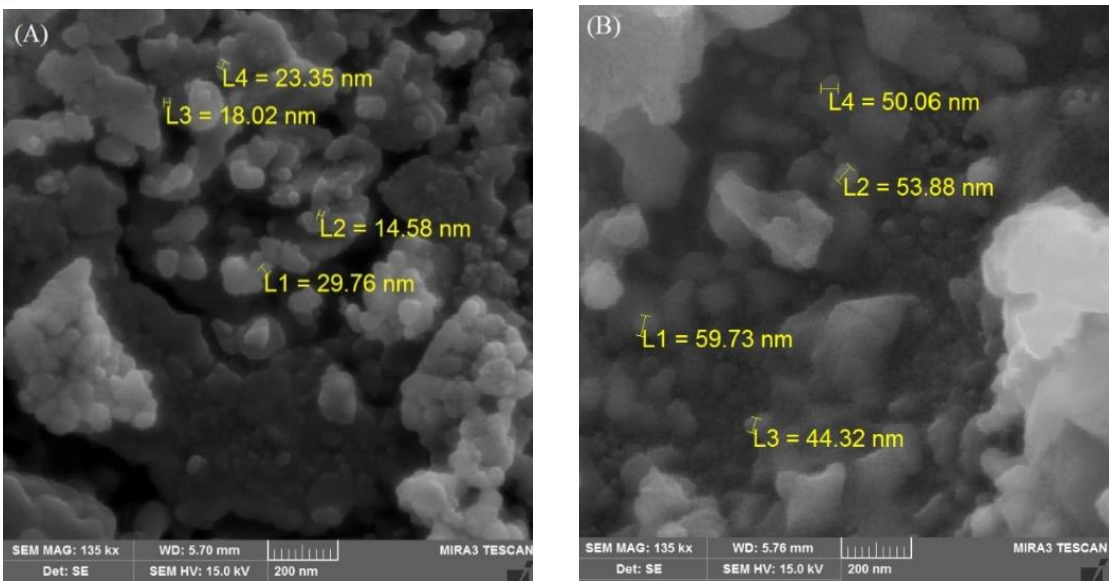

Fig. (5) SEM microimages of prepared HAp powder prepared at (A) 600°C and (B) 800°C

The exact qualities and the desired properties of the HAp would determine the ideal calcination temperature to reach the maximum microhardness. Table (1) shows that the microhardness increased with increasing sintering temperature.

The Young's modulus, which refers to the material's stiffness or elasticity and quantifies how stress and strain interact during deformation, was determined. This modulus of HAp can be influenced by the calcination temperature, which can also alter the crystal structure, grain size, and porosity of the prepared material.

Table (1) shows values of some mechanical parameters as a function of sintering temperature. The Young's modulus of the prepared HAp typically increase, similar to microhardness, with increasing sintering temperature. A more rigid structure is produced as a result of better crystallinity being promoted by higher sintering temperatures. As a result, at higher temperatures, the Young's modulus has a tendency to be larger.

Table (1) Values of some mechanical parameters as a function of sintering temperature

Sintering Temperature (°C)	V_l (m/s)	V_T (m/s)	Bulk density (kg/m^3)	Vickers Hardness (GPa)	Young's Modulus (GaP)	K_{IC} (MPa /m$^{1/2}$)
600	3464.2	2313	1862	4.2	1.205	2.828
800	3772.1	2494	2442	7.4	2.105	4.606

4. Conclusions

This work involved the chemical synthesis of hydroxyapatite (HA) powder and analysis of the effect of calcination temperature on the crystalline structure of the material. The prepared HA powder was polycrystalline. The average crystallite size of the prepared powder calcined at 800°C was determined to be 36.27 nm. The particle size was found to increase with increasing calcination temperature. Also, Vickers microhardness and Young's modulus were both increasing with temperature, showing enhanced crystallinity and stiffness. The findings of this work may contribute to the understanding of production, characterization, and potential applications of HA powder in biomedical fields.

References

[1] Y. Javad et al., "A short view on nanohydroxyapatite as coating of dental implants", *Biomed. Pharmacother.*, 105 (2018) 553-557.

[2] A.N. Lipton, A. Fathima and S.G.P. Vincent, "In-vitro Evaluation of Chitosan-Hydroxyapatite Nanocomposite Scaffolds as Bone Substitutes with Antibiofilm Properties", *J. Pure Appl. Microbiol.*, 15(3) (2021) 1455-1471.

[3] F. Elisa et al., "Hydroxyapatite for Biomedical Applications: A Short Overview", *Ceramics*, 4 (2021) 542-563.

[4] S. Pokhrel, "Hydroxyapatite: Preparation, Properties and Its Biomedical Applications", *Adv. Chem. Eng. Sci.*, 27 (2018) 225-240.

[5] G.C. Koumoulidis et al., "Preparation of hydroxyapatite nanoparticles using a modified precipitation method", *Demokritos National Centre for Scientific Research, Institute of Materials Science*, 156 (2003) 10, 83-90.

[6] S. Ramesh et al., "Sintering properties of hydroxyapatite powders prepared using different methods", *Ceram. Int.*, 39(1) (2013) 111-119.

[7] M. Guoqing, "Three common preparation methods of hydroxyapatite", *Mater. Sci. Eng.*, 688 (2019) 033057, 1-12.

[8] L. Sopyan, R. Singh and M. Hamdi, "Synthesis of nano sized hydroxyapatite powder using sol-gel technique and its conservation to dense and pours bodies", *Indian J. Chem.*, 47A(11) (2008) 1626-1631.

[9] A.J. Ruys et al., "Sintering effects on the strength hydroxyapatite", *Biomater.*, 16 (1995) 409-415.

[10] Z.Y. Li et al., "Chemical composition, crystal size and lattice structural changes after incorporation of strontium into biomimetic appetite", *Biomater.*, 28 (2007) 1452-1460.

[11] Y. Waseda, E. Matsubara and K. Shinod, **"X-Ray Diffraction Crystallography"**, Springer (Heidelberg, 2011).

[12] I. Uysal et al., "Co-doping of hydroxyapatite with zinc and fluoride improves mechanical and biological properties of hydroxyapatite", *Prog. Nat. Sci. Mater. Int.*, 24(4) (2014) 340-349.

[13] B.D. Cullity, **"Elements of X-ray Diffraction"**, Addison-Wesley Pub. Co., Inc. (1978).

[14] A. Benhammou et al., "Mechanical behavior and ultrasonic non-destructive characterization of elastic properties of cordierite-based ceramics", *Ceram. Int.*, 39(1) (2013) 21-27.

[15] G.R. Anstis et al., "A Critical Evaluation of Indentation Techniques for Measuring Fracture Toughness: I, Direct Crack Measurements", *J. Am. Ceram. Soc.*, 64(9) (1981) 533-538.

[16] R.F. Cook, "Direct Observation and Analysis of Indentation Cracking in Glasses and Ceramics", *J. Am. Ceram. Soc.*, 73(141) (1990) 787-817.

[17] A. Hanifi and M.H. Fathi, "Bioresorbability Evaluation of Hydroxyapatite Nanopowders in a Stimulated Body Fluid Medium", *Iranian J. Pharmaceut. Sci.*, 4(2) (2008) 141-148.

[18] I. Uysal et al., "Co-doping of hydroxyapatite with zinc and fluoride improves mechanical and biological properties of hydroxyapatite", *Prog. Nat. Sci. Mater. Int.*, 24(4) (2014) 340-349.

 ISSN (print) 2958-8960 (online) 3006-6042 Printed in IRAQ